KSTLE International Journal, Vol. 1, No. 1, June 2000, pp. 12-20

Nano-Wear and Friction of Magnetic Recording Hard Disk by Contact Start/Stop Test

Woo Seok Kim[1], Pyung Hwang[1,*] and Jang-Kyo Kim[2]

[1]*School of Mechanical Engineering, Yeungnam University*
[2]*Hong Kong University of Science and Technology, Department of Mechanical Engineering*

Abstract : Nano-wear and friction of carbon overcoated laser-textured and mechanically-textured computer hard disk were characterised after contact start/stop (CSS) wear test. Various analytical and mechanical testing techniques were employed to study the changes in topography, roughness, chemical elements, mechanical properties and friction characteristics of the coating arising from the contact start/stop wear test. These techniques include: the atomic force microscopy (AFM), the continuous nano-indentation test, the nano-scratch test, the time-of-flight secondary ion mass spectroscopy (TOF-SIMS) and the auger electron spectroscopy (AES). It was shown that the surface roughness of the laser-textured (LT) bump and mechanically textured (MT) zone was reduced approximately 4nm and 7nm, respectively, after the CSS wear test. The elastic modulus and hardness values increased after the CSS test, indicating straining hardening of the top coating layer. A critical load was also identified for adhesion failure between the magnetic layer and the Ni-P layer. The TOF-SIMS analysis also revealed some reduction in the intensity of C and C_2F_5, confirming the wear of lubricant elements on the coating surface.

Key words : nano-wear, contact start/stop, laser-texture, mechanically-texture, surface roughness, friction behaviour, interface failure

Introduction

As the recording density of computer hard disk has increased tremendously in recent years, the magnetic flying height of the recording head over the data zone needs to be decreased. The reduction in flying height inevitably introduces many unwanted side effects: direct contact between the head and disk often leads to nano-wear of surface coating and increase in stiction and friction with increasing the contact start/stop cycles, degrading the function of head/disk interface. The introduction of laser texture (LT) technique makes it possible to precisely control the topography of the landing zone by creating discrete topographical features with round, dome-like protrusions, usually known as bumps, on the start/stop zone [1-4]. The disks containing LT zones can offer a low cost, high precise control of the surface topography and zone position. The presence of LT bumps was shown to improve significantly the tribological performance in contact start/stop testing and glide avalanche prediction [5]. For the LT zone, the stiction remained almost constant and the statistical wear rate was much lower than the MT zone for the same range of CSS cycles, because the stiction force at the MT zone was much higher than that at the LT zone [6]. This was despite the fact that the acoustic emission signal of LT disks was generally higher than that of MT disks. The shape, radius, height and location of these bumps can be accurately controlled by controlling laser parameters, such as laser pulse energy, pulse width and laser wave length [7]. A smaller focus spot size and shorter pulse width produced a smaller radius of rim curvature, which in turn is beneficial in reducing stiction [4].

A significant progress has been made of nano-tribology of these magnetic coating systems [8]. Sliding wear mechanisms that are potentially operative in contact recording are sensitive to the mechanical properties of the surface coatings, such as shear strength, hardness, elastic modulus, and fracture toughness, as well as surface roughness, topography and friction. These properties of various coatings have been characterized using state-of-the-arts techniques, such as nano-indentation, nano-scratch techniques, atomic force microscopy (AFM) [9-11], and stylus profilers and non-contact optical profilers were used to measure surface roughness [12,13]. In addition to the above instruments, Raman spectroscopy was also successfully used to study the morphology of ultra-thin carbon films of thickness down to 1nm, as well as to identify the non-uniformity in the wear rates along the air bearing surface [14]. Surface analytical techniques, such as time-of-flight secondary ion man spectroscopy (TOF SIMS), X-ray photoelectron spectroscopy (XPS), Auger depth profiling [15-17], have become much widely used to evaluate the wear mechanisms and durability of various ultra-thin films and textures. The point contact microscopy [18] was also used to conduct nano-wear tests.

The present work is a continuation of our previous study [19] on anisotropic tribological and mechanical properties of mechanically textured disk surface. The nano-wear mecha-

*Corresponding author; Tel: 82-53-810-2448, 813-7690
Fax: 82-53-813-3703; E-mail: phwang@yu.ac.kr

nism, friction behavior, coating failure characteristics and other tribological properties of both the laser and mechanically textured disks are studied before and after contact start/stop cyclic wear tests. Special emphasis was placed on evaluation of the changes in surface chemistry characteristics and adhesion failure mechanisms between the coatings that were caused by the contact cyclic wear.

Experimental Procedure

Materials and Contact Start/Stop (CSS) Wear Test

Two types of textured disk surface were employed in this study: laser-textured (LT) disk containing arrays of small bumps introduced on the start/stop zone; and mechanically-textured (MT) disk. Both the disks consisted of Al-Mg alloy 5086 substrate (95.4% Al, 4% Mg, 0.4% Mn, and 0.15% Cr) which was electroless-plated with a 10-20 μm thick Ni-P layer to improve the surface hardness [20]. A magnetic Co-Cr-Ta layer of 70-100 nm in thickness was deposited, on top of which an amorphous carbon coating of 20-30 nm and Z-Dol lubricant of 2-4 nm in thickness were placed to protect the magnetic layer [21].

Wear tests were conducted with the standard contact start/stop (CSS) testing machine. Fig. 1 presents the schematics of CSS tester, and the acceleration profile used in the experiment. Each CSS cycle was 11.2 s at a maximum spindle speed of 5400 rpm, which corresponded to a linear velocity of approximately 7.1 m/s. Both the LT and MT disks were subjected to 15 K cycles in a clean room at ambient temperature. The head slider type is negative pressure tri-pad slider and its load is 3.0 g. The disk surface was examined before and after the CSS wear test using the several characterization techniques as described below.

Atomic Force Microscopy and Surface Roughness Analysis

The surface roughness was measured and the topographic images of disk were taken on an atomic force microscope (AFM, TMX2000, Discovery Probe microscope, TopoMetrix). A piezoelectric (PZT) tube scanner was used to scan the sample in three-dimension with nanometer resolution at a rate of 40 μm/s. Three regions were chosen for scanning and the scan size was 20 μm × 20 μm square for the LT bump and MT zone. The measurement of surface roughness of LT bumps were much more difficult than the flat surfaces of MT zone, because the height along the bump top area was irregular and the bump height did not relate to the texture direction around the bump. Therefore, a new method was devised to overcome these problems, by scanning the bump top following lines through the center of bump at 10° intervals. Eight bumps were randomly chosen from the start/stop zone for scanning. Line analyses were performed of the peak-to-valley distance, v, (or the depth) for the LT bump and the peak-to-mean distance, m, for the MT zone. The surface roughness data thereby obtained were treated statistically based on both the Weibull cumulative distribution function, $F(x)$, and the probability density function, $f(x)$ [19]:

$$F(x) = 1 - exp\left[-\left(\frac{x}{\theta}\right)^b\right] \tag{1}$$

$$f(x) = \frac{b}{\theta^b} x^{b-1} exp\left[-\left(\frac{x}{\theta}\right)^b\right] \tag{2}$$

where b is the shape parameter (or Weibull modulus), and θ is the scale parameter.

Nano-indentation and Nano-scratch tests

The Nano-indentation and nano-scratch tests were performed to measure the hardness and elastic modulus as well as the adhesion characteristics using a nano-indenter (Nanoindenter II by Nano Instrument Inc.) [22]. The indenter is equipped with a three-sided pyramidal Berkovich diamond indenter tip with a tip radius less than 100 nm. During indentation, the instrument monitors and records the dynamic load and displacement of the indenter tip. The 'continuous stiffness mode' was used where an incremental load was applied continuously until the displacement reached a desired value of 500 nm [23]. The output response provided the stiffness and contact area data without discrete unloading cycles. Indentation was performed before and after 15 K CSS wear test and three different positions were indented for a given LT bump, namely outside, on the bump.

The nano-scratch tests were conducted to study the friction characteristics and coating-substrate adhesion of the disk surface before and after the CSS wear tests. The 'ramp load mode' was employed with an increasing load from 0 mN to 10 mN at a rate of 100 μN/s. The Berkovich diamond tip was scratched in the face-forward direction, i.e. with the face of the tip facing the scratch direction. After the scratch tests, the topographic images of scratch deformation and depth were generated using the AFM.

Surface Analysis

The time-of-flight secondary ion mass spectroscopy (TOF-SIMS, PHI 7200 from Physical Electronics, Inc.) and Auger electron spectroscopy (AES, PhI 5600 Physical Electronics Multi-Technique System) were employed to identify the changes in surface chemical and atomic compositions after the CSS wear test. In the TOF-SIMS analysis, a pulsed primary ion beam is sputtered on the top surface layer of the material, and the secondary ions emitted from the surface are analyzed using a time-of flight mass spectrometer. The sampling depth of TOF-SIMS was in the range of 10 to 20Å, since only the particles in the outermost region of a sample had sufficient energy to overcome the surface binding energy and leave the sample. The AES instrumentation involved a UVH system, electron gun for target excitation and an electron spectrometer for energy analysis of emitted electrons. The Auger analysis was conducted on the disk surface for 12 min. in a depth-profiling mode. The primary electron energy used was 5.0 keV with a beam current of 0.5 μA, and the beam was focused to a spot diameter of about 2 mm. If any damage has occurred at the start/stop zone due to the depletion of the carbon coating or lubricant, the changes can be detected by the surface chemistry.

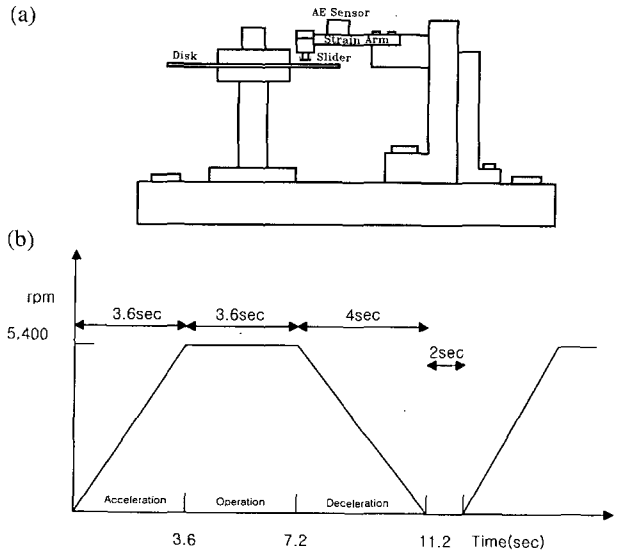

Fig. 1. Schematics of (a) contact start/stop wear tester and (b) acceleration profile of the CSS wear test.

Results and Discussion

Surface Roughness

Major findings from the experiments are summarised in the following. Discussions are made of the wear and failure mechanisms of LT and MT disk surfaces after the CSS wear test. Typical AFM 3 D topographic images of the LT bump and MT zone before and after the CSS wear test are presented in Figs. 2 and 3, respectively. There were some clear indications of nano-wear after the CSS wear test depending on the type of textures. A number of small debris-most likely of carbon coating-were detected inside the bump (Fig. 2(b)), indicating that significant nano-scale wear took place between the head and the disk. Comparison of Figs. 3(a) and (b) also suggests that the roughness of the MT zone be to a certain extent reduced after the CSS wear test. The cumulative probability distributions according to the Weibull and probability density distributions presented in Fig. 4 further support the above findings. The Weibull parameters, b and θ, were calculated before and after the CSS wear test, and are summarised in Table 1. It is obvious that both the average values and the scattering of surface roughness decreased, as evidenced by the increase in shape parameter, b, and reduction in scale parameter, θ, after the CSS wear test. The changes in these roughness parameters were much more remarkable for the MT zone than for the LT bumps, strongly indicating a more serious nano-wear in the former surface. The reductions in the mean value were approximately 7nm and 4nm, respectively, after 15 k CSS test. Similar conclusions can be drawn from the probability density distributions (Figs. 4(c) and (d)).

Elastic Modulus and Hardness

The elastic modulus and hardness values measured from the nano-indentation tests are plots as a function of indentation depth in Figs. 5 and 6, respectively. It is interesting to note that for the LT bump, these mechanical properties were slightly

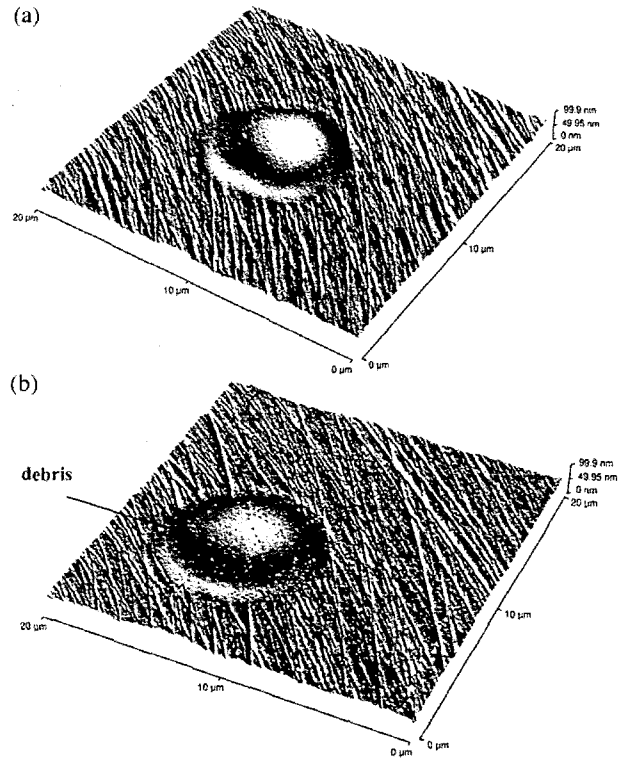

Fig. 2. AFM images of laser textured bump (a) before and (b) after the CSS wear test.

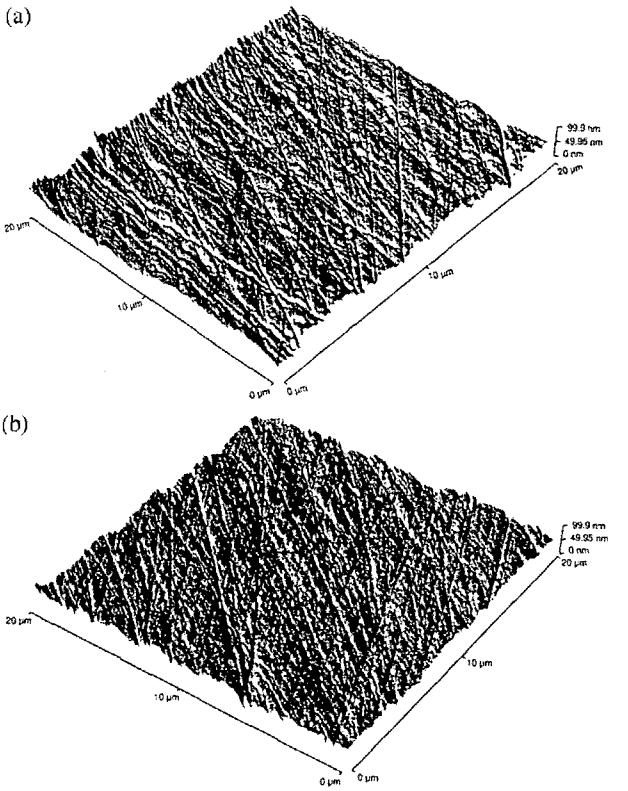

Fig. 3. AFM images of mechanically textured zone (a) before and (b) after the CSS wear test.

higher at the top of bump than the other areas surrounding the bump (Fig. 5(a) and 6(a)). However, it was rather difficult to

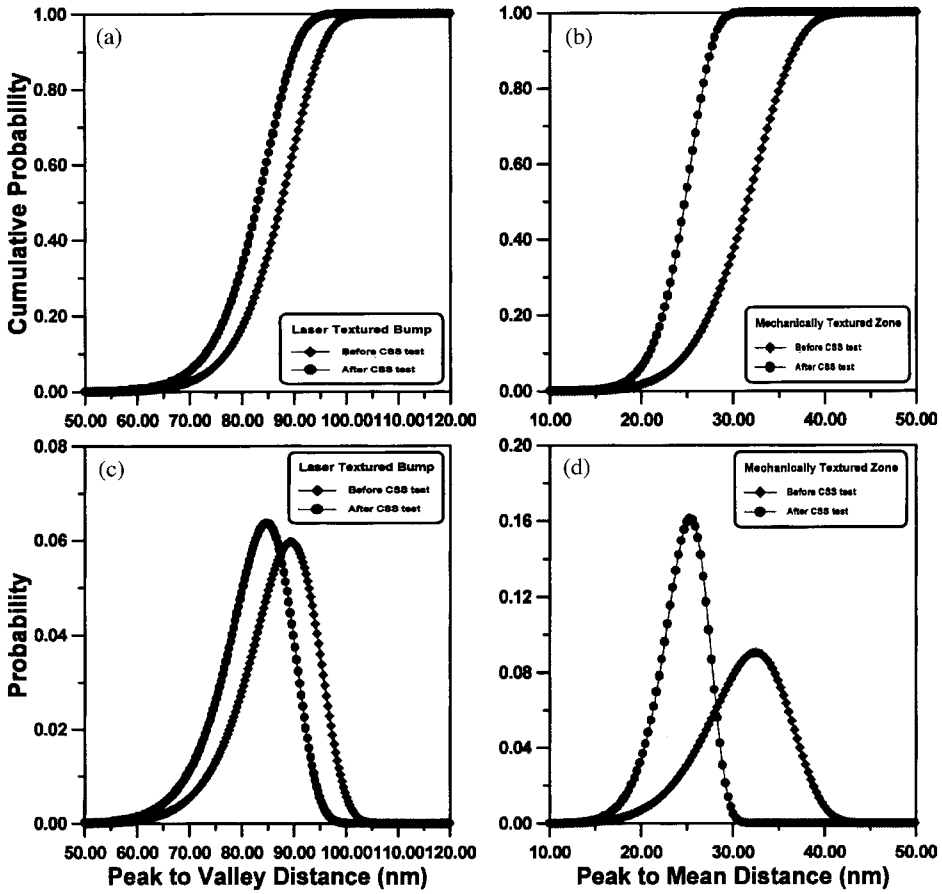

Fig. 4. (a), (b)Weibull cumulative and (c), (d)probability density distributions of surface roughness.

detect any variations of these properties after the CSS wear test. In contrast, the initial values of the elastic modulus and hardness of MT zone at low indentation depths were much higher after the CSS wear test than before it (compare Figs. 5(c) and 6(c) with Figs. 5(d) and 6(d)). This may indicate that after the contact start/stop wear test, the carbon coating became denser and harder, giving rise to a high elastic modulus and hardness. It is also likely that the magnetic coating and the Al-Mg alloy substrate underwent strain hardening due to the contact stresses and the generation of internal stress fields [24]. This observation is quite congruent with the significant reduction in surface roughness of the MT zone, as discussed above. It appears that the effect of plastic deformation was restricted only to the top layer less than approximately 150~200 nm from the surface, as indicated by the unchanged properties when the indentation was continued to a large depth.

Coefficient of Friction and Scratch Depth

The coefficients of friction measured from the nano-scratch test are plotted as a function of normal load before and after the CSS wear test, as shown in Fig. 7. They increased rapidly at the initial ramp loading, which was followed by a slow increase with further increase in applied load. Especially, the MT zone exhibited approximately a bi-linear relationship between the coefficient of friction and normal load. There was invariably a sudden surge or drop of coefficient of friction, when the applied load reached approximately 9.5 mN, for all conditions tested. Basically the identical results were obtained from the scratch depth versus normal load plots, as shown in Fig. 8. The sudden increase or drop of coefficient friction is thought to be a direct reflection of the changes in vertical displacement of the indenter tip while scratching in the ramp load mode. The load corresponded to a scratch depth of about 140nm, which is roughly equal to the depth of interface between Co-Cr-Ta magnetic layer and Ni-P layer. Judging from this information, the abrupt change in indenter depth was most likely attributed to the fracture of the interface bond between Co-Cr-Ta magnetic layer and Ni-P layer. It is also

Table 1. Weibull parameters: shape parameter, b and scale parameter, *θ*.

Weibull Parameters	LT bump before CSS test	LT bump After CSS test	MT zone before CSS test	MT zonee after CSS test
Shape Parameter, b	14.5	14.7	8.06	11.2
Scale Parameter, θ	89.8	85.2	33.0	25.6

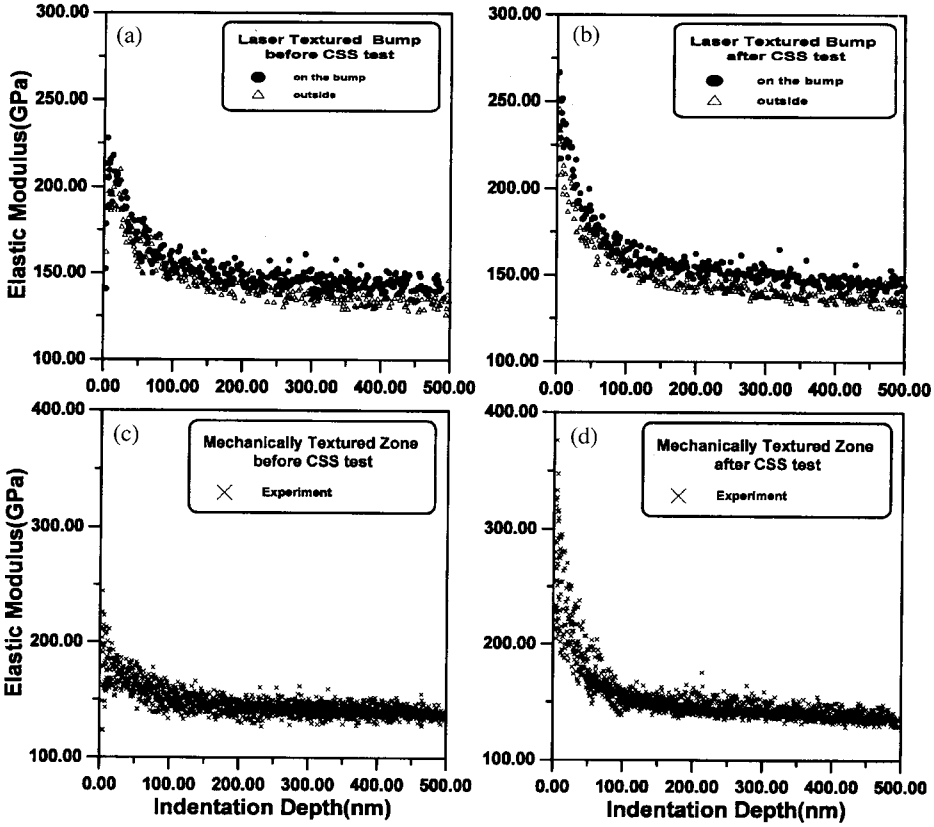

Fig. 5. Elastic Modulus of (a), (b) laser textured bump, and (c), (d) mechanically textured zone as a function of indentation depth.

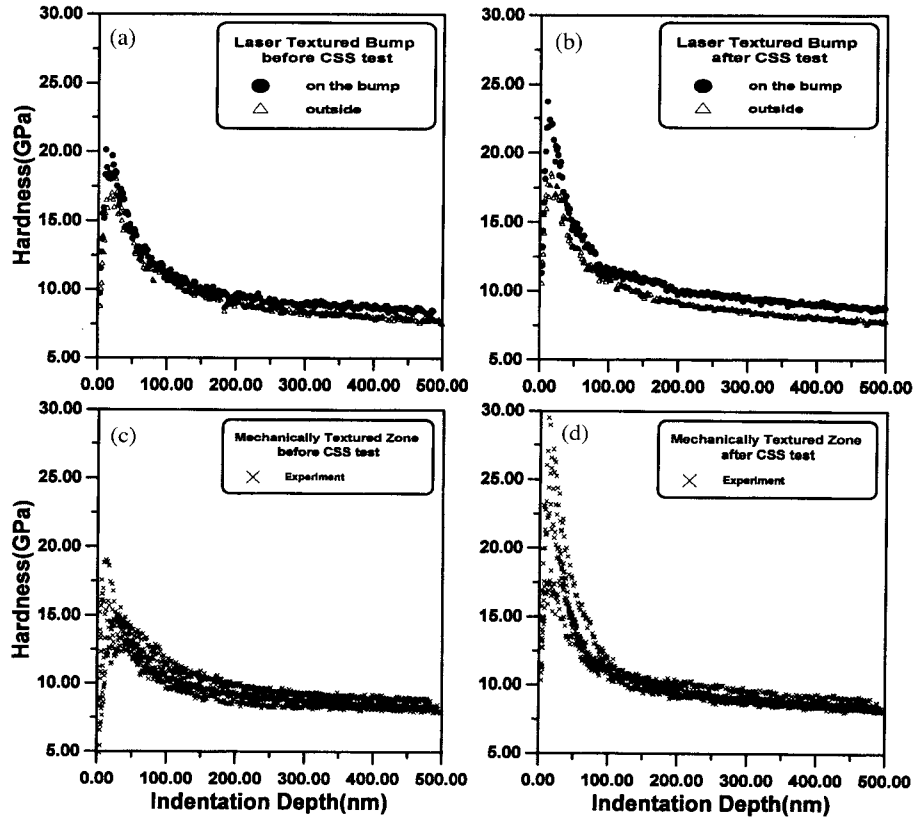

Fig. 6. Hardness of (a), (b) laser textured bump, and (c), (d) mechanically textured zone as a function of indentation depth.

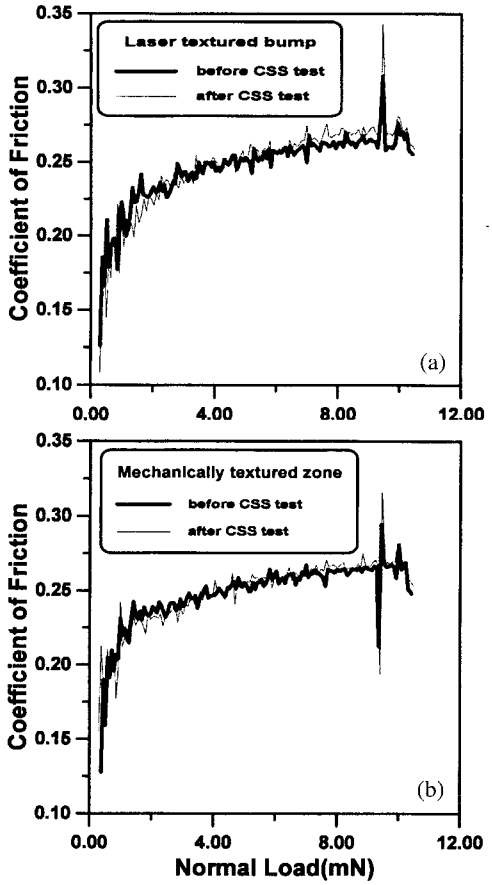

Fig. 7. Coefficient of friction as a function of normal load for laser textured bump before and after the CSS test(a); and for mechanically textured zone before and after the CSS test(b).

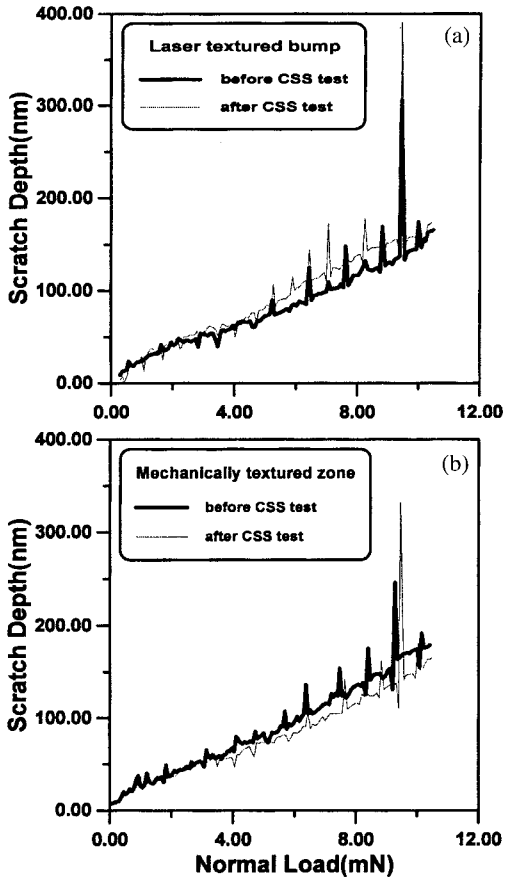

Fig. 8. Scratch depth as a function of normal load for laser textured bump before and after the CSS test(a); and for mechanically textured zone before and after the CSS test(b).

worth noting that for both the LT bump and MT zone, the abrupt changes in coefficient of friction or scratch depth were more severe after the CSS wear test than before it. It is expected that for both the LT bump and MT zone, the interface bond between the two coatings became weaker with increasing the number of CSS wear cycles. This seems quite consistent with the higher initial elastic modulus and hardness values after the CSS wear test than before it (Figs. 5 and 6).

Surface Elemental Analysis

The mass spectra obtained from the TOF-SIMS experiments are illustrated in Fig. 9. It was noted that for both the LT bump and MT zone, the intensities of C(12), C_2H_7(31), CFO(47), CF_2(50), CF_3(69), C_2F_3(81), C_2F_4(100), C_2F_5(119) all decreased substantially after the CSS wear test. These elements are identified as the chemicals of Z-Dol, the lubricant applied on the surface of disk coating. This means that the reduction was mainly attributed to the local depletion of the lubricant, Z-Dol. It should be mentioned here that C(12) is not carbon coating, but belongs to the lubricant element. It is also interesting to note that the reductions of the intensities of the above chemicals were more remarkable for the MT zone than for the LT bump, a clear indication that the MT zone is more susceptible to nano-wear. This observation is considered to be quite consistent with the results presented in the foregoing sections based on other techniques. Typical TOF-SIMS 2D intensity maps for the LT bump surface are presented in Fig. 10. It is clearly seen that there were significant drops in the intensities of the masses, C(12) and C_2F_5(119) after the CSS wear test. A similar conclusion was drawn for the reduction of lubricant level on the bump due to the reduction of TOF SIMS signal from C_2F_5(119) after 25k CSS test [25].

The AES spectra presented in Fig. 11 did not reveal any significant changes between before and after the CSS wear test. No elements from the magnetic layer were detected, and only carbon coating elements were shown. The spectra were practically identical for the LT and MT disk surfaces. This does not mean that there was no wear taking place, but rather indicates that the AES was not particularly sensitive enough to detect the type of wear occurred. This seems because the wear was limited mainly to the lubricant, and some reduction of surface roughness due to the internal plastic deformation occurred in the underlying coating materials.

Concluding Remarks

To assess the nano-wear and friction mechanism on the carbon coating of magnetic recording media after contact start/stop

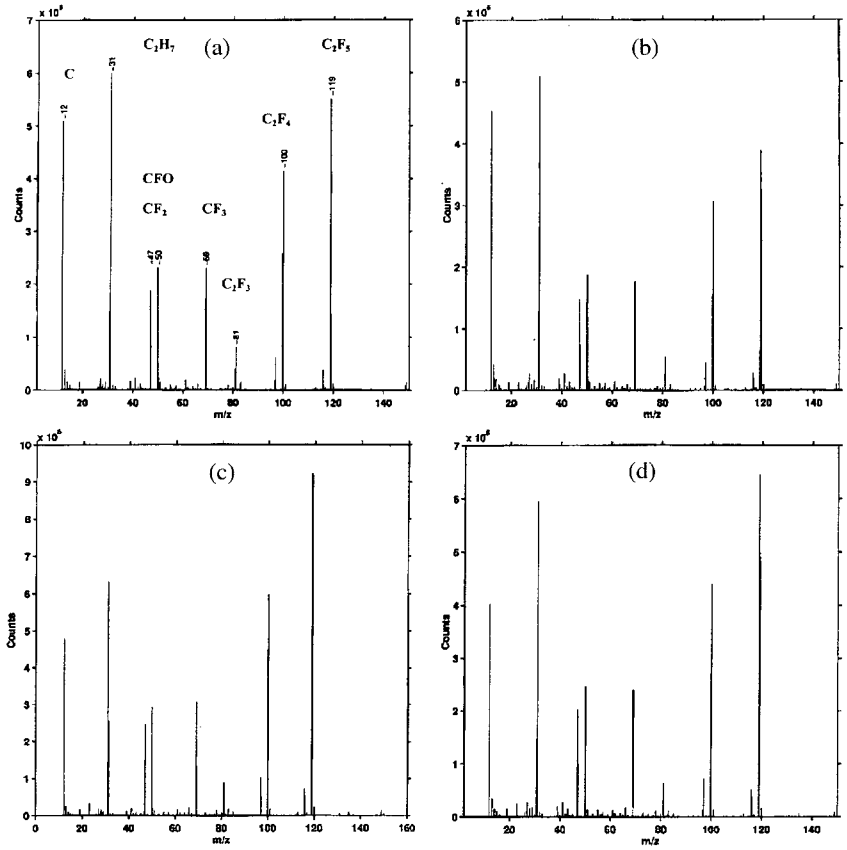

Fig. 9. TOF-SIMS mass spectra for surface elements of laser textured bump (a) before and (b) after the CSS test; and for mechanically textured zone (c) before and (d) after the CSS test.

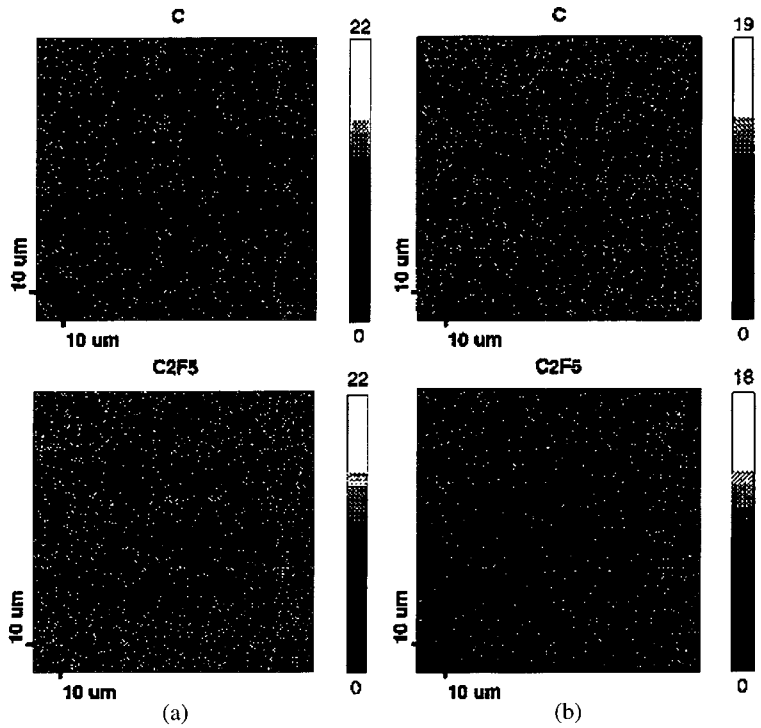

Fig. 10. TOF-SIMS 2D intensity maps for surface lubricant elements, C and C_2F_5 of laser textured bump (a) before and (b) after the CSS wear test.

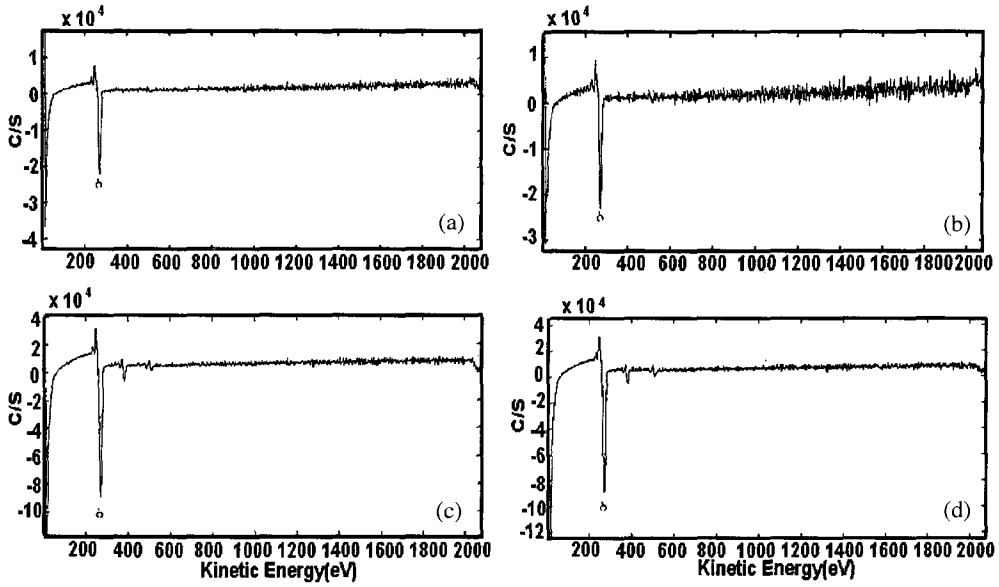

Fig. 11. AES surface intensity as a function of kinetic energy for laser textured bump (a) before and (b) after the CSS test; and mechanically textured zone (c) before and (d) after the CSS test.

wear test, various mechanical and analytical experiments have been performed, including atomic force microscopy, nano-indentation and nano-scratch tests, time-of-flight secondary ion mass spectroscopy and Auger electron spectroscopy. The following can be summarised.

(i) The AFM images did reveal some local nano-wear on the carbon coating after the CSS wear test. The surface roughness was reduced by about 4 nm and 7 nm after the CSS wear test of 15 K cycles on the laser textured (LT) bump and mechanically textured (MT) zone, respectively.
(ii) The elastic modulus and hardness of the LT bump top were slightly higher than other surrounding regions, probably as a result of strain hardening introduced by the laser texturing process. For the MT zone, these properties obtained after the CSS wear test at a shallow indentation depth were much higher than before the test. This is attributed to strain hardening of the top coating layer arising from contact stresses and the generation of internal stress fields during the CSS wear test.
(iii) The scratch depth and the corresponding coefficient of friction displayed sudden surge or drop at a normal load of approximately 9.5 mN (or equivalent scratch depth of about 140 nm) during the nano-scratch test for all conditions studied. The characteristic sudden change in scratch behavior was interpreted as the failure of adhesion between the magnetic layer and the underlying Ni-P layer.
(iv) The TOF-SIMS spectra displayed significant reductions in the intensities of lubricant elements, such as C(12), C_2H_7(31), CFO(47), CF_2(50), CF_3(69), C_2F_3(81), C_2F_4(100), C_2F_5(119), after the CSS wear test. This is attribute to contact wear at the head/disk interface. The 2D intensity maps confirmed the above findings for the elements C(12) and C_2F_5(119). The AES was not particularly sensitive enough to detect the type of wear observed above.

Acknowledgments

The authors wish to thank Samsung Electronics for the supply of hard disks and carrying out the CSS wear experiments. WSK was a visiting scholar from Yeungnam University, Korea to Hong Kong University of Science & Technology (HKUST), Hong Kong when this work was performed. Most experiments were conducted with the technical supports of the Material Characterization & Preparation Facilities (MCPF) and the Advanced Engineering Materials Facilities (AEMF) at HKUST. The financial support from the HK Research Grant Council (RGC) and the Area of Excellent (AoE) Grant from HKUST are also acknowledged.

References

1. Ranjan, R., Lambeth, D. N., Tromel, M., Goglia, P. and Li, Y., Laser texturing for low-flying height media, J. Appl. Phys. 69, pp. 5745-5747, 1991.
2. Baumgart, P., Krajnovich, D. J., Nguyen, T. A. and Tam, A. C., A New Laser Texturing Technique for High Performance Magnetic Disk Drives, IEEE Trans. Mag., Vol. 31, No. 6, pp. 2946-2951, 1995.
3. Kuo, D., Gui, J., Marchon, B., Lee, S., Boszormenyi, I., Liu, J. J., Rauch, G. C. and Vierk, S., Design of laser zone texture for low glide media, IEEE Trans. on Magnetics, Vol. 32, pp. 3753-3758, 1996.
4. Liu, J. J., Optimization of Laser Texture for the Head-Disk Interface, IEEE Trans. Mag., Vol. 33, No. 5, pp 3202-3204, 1997.
5. Marchon, B., Kuo, D., Lee, S., Gui, J. and Rauch, G. C., Gliding avalanche prediction from surface topography, Trans. ASME, J. Tribology, Vol. 118, No. 3, pp.644-650, 1996.
6. Khurshudov, A., Knigge, B. and Talke, F. E., Tribology of Laser-Textured and Mechanically-Textured Media, IEEE Trans. Mag., Vol 33, pp. 3190-3192, 1997.

7. Chilamakuri, S. and Bhushan, B., Effect of peak radius on design of W-type donut shaped laser textured surfaces, Wear, Vol. 230, pp. 118-123, 1999.
8. Bhushan, B., Tribology and Mechanics of Magnetic Storage Devices, Springer, New York, 1996.
9. Bhushan, B., Gupta, B. K. and Azarian, M. H., Nano-indentation, Microscratch, Friction and Wear Studies of Coatings for Contact Recording Applications, Wear, Vol. 181-183, pp. 743-758, 1995.
10. Wei, B., Komvopoulos, K., Nanoscale Indentation Hardness and Wear Characterization of Hydrogenated Carbon Thin Films, ASME Journal of Tribology, Vol. 117, pp. 594-601, 1995.
11. Xuan, J., Shih, C., Feng, Z., Peng, G. and Nguyen, T., A Study on Nano-Wear at Laser-Textured Bump Tips and The Failure Mechanism at the Head-Bump-Interface, IEEE Trans. Mag., Vol. 33, No. 5, pp. 3187-3189, 1997.
12. Poon, C. Y. and Bhushan, B., Surface roughness analysis of glass-ceramic substrates and finished magnetic disks, and Ni-P coated Al-Mg and glass substrates, Wear, Vol. 190, pp. 89-109, 1995.
13. Tanaka, H., Ishikawa, F., Gomi, K., Yamaguchi, N. and Miyake, Y., Tribological behaviour of thin film rigid disks with regular dot array texture on carbon overcoats, IEEE Trans. Mag., Vol. 30, pp. 4113-4115, 1994.
14. Varanasi, S. S., Lauer, J. L., Talke, F. E., Wang, G. and Judy, J. H., Friction and wear studies of carbon overcoated thin films magnetic sliders: application of Raman microscopy, Trans. ASME, J. Tribology, Vol. 119, 471-475, 1997.
15. Machcha, A. R., Azarian, M. H. and Talke, F. E., An Investigation of Nano-Wear during Contact Recording, Wear, Vol. 197, pp. 211-220, 1996.
16. Bhushan, B., and Cheng Y., Wear and degradation mechanisms of magnetic thin-film rigid disks with different lubricants using mass spectrometry, J. Appl. Phys., 81(8), 15 April, 5390-5392, 1997.
17. Miyamoto, T., Sato, I., and Ando, Y., Friction and Wear Characteristics of Thin Film Disk Media in Boundary Lubrication, Tribology and Mechanics of Magnetic Storage Systems, STLE SP-25, pp. 55-59, 1998.
18. Jiang, Z., Lu, C. J., Bogy, D. B. and Miyamoto, T., An investigation of the experimental conditions and characteristics of a nano-wear test, Wear, Vol. 181-183, pp. 777-783, 1995.
19. Kim, D. H., Hwang, P. and Kim, J. K., Anisotropic Tribological properties of the coating on a magnetic recording disk Thin Solid Films, Vol. 360, pp. 187-194, 2000.
20. Yamaguchi, H., Tsukamoto, Y., and Yanagisawa, M., Mechanical Properties and Durability of Sputtered Carbon Protective Overcoats for Rigid Magnetic Disks, Tribology and Mechanics of Magnetic Storage Systems, Vol. V, STLE SP-25, pp. 82-86, 1988.
21. Ishihara, H., Yamagami, H., Sumiya, T., and Okudera, M., Contact start/stop characteristics on photolithographic magnetic recording media, Wear, Vol. 172, pp. 65-72, 1994.
22. Tsui, T. Y., Pharr, G. M., Oliver, W. C., Bhatia, C. S., White, R. L., Anders, S., Anders, A., and Brown, I. G., Nanoindentation and Nanoscratching of Hard Carbon Coating for Magnetic Disks, Mat. Res. Soc. Symp. Proc., Vol. 383, Drory, M. D., Bogy, D. B., Donley, M. S., and Field, J. E. (eds.), pp. 447-452, 1995.
23. Kim, D. H., Kim, J. K., Sham, M. L. and Hwang, P., Indentation properties on copper leadframe with hard coatings Metal. Mater. Vol. 4, pp. 812-817, 1998.
24. Czichos, H., Tribology, Chap. 5, Elsevier Scientific Publishing Com., 1978.
25. Wang, R. H., Raman, V., Baumgart, P., Spool, A. M. and Deline, V., Tribology of Laser Textured Disks with thin overcoat, IEEE Trans. Mag., Vol. 33, No. 5, pp. 3184-3186, 1997.